KARYA ILHAM PUBLISHING
CONNECTING MINDS, BRIDGING IDEAS, INSPIRING READERS

Future Energy and Environment Letters

Journal homepage:
https://karyailham.com.my/journals/index.php/feel/index
ISSN: 3083-8940

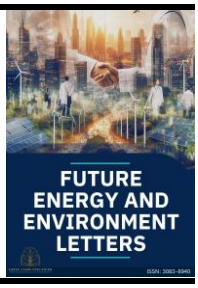

Enhancing Biodegradability and Functionality of Packaging Films: A Statistical Approach of Sago Starch Nanocomposite

Basirah Fauzi[1,2,*], Mohd Ghazali Mohd Nawawi[2], Roslinda Fauzi[3], Nurul Izzati Mohd Ismail[1], Dilaeleyana Abu Bakar Sidik[1], Nur Shahirah Mohd Aripen[1], Faridatul Ain Mohd Rosdan[4], Dzulhilmi Kamarudin Sohami[5]

[1] Department of Science and Mathematics, Centre for Diploma Studies, Universiti Tun Hussein Onn Malaysia, 84600 Pagoh, Johor, Malaysia
[2] Department of Chemical Engineering, Faculty of Chemical and Energy Engineering, Universiti Teknologi Malaysia, 81310 Skudai, Johor, Malaysia
[3] School of Industrial Technology, Faculty of Applied Sciences, Universiti Teknologi MARA, 40450 Shah Alam, Selangor, Malaysia
[4] School of Chemical and Process, University of Leeds, LS2 9JT, United Kingdom
[5] BASF (Malaysia) Sdn.Bhd., Petaling Jaya, Selangor, Malaysia

ARTICLE INFO

Article history:
Received 30 November 2024
Received in revised form 7 December 2024
Accepted 15 December 2024
Available online 26 December 2024

Keywords:
Optimization; sago starch; chitosan nanoparticles; polyvinyl alcohol; film

ABSTRACT

The attractive factors of starch as a packaging material are its low price and degradable properties. However, brittleness hindered the starch from functioning well as a packaging film. Researchers have done a few studies about numerous types of starch but have had no reports on sago starch (SS). The incorporation of polyvinyl alcohol (PVA) and chitosan nanofillers (CSN) into SS formulations was aimed at improving mechanical properties. Synthesis of packaging film was then formulated by Design Expert 13.0 with three independent variables, which were compositions of sago starch (SS), chitosan nanoparticles (CSN), and polyvinyl alcohol (PVA) at 100 wt % of solution basis. Seventeen experimental designs produced the probability error of tensile strength and swelling index at $p < 0.05$. The ANOVA shows that both responses give the p-value at 0.0177 and 0.0106, respectively. This has confirmed that the optimization of film formulation has been achieved accordingly.

1. Introduction

The production and widespread use of nondegradable plastics exacerbate waste disposal challenges [1]. This issue arises partly because consumers are not adequately exposed to measures for preventing pollution. In recent decades, there has been a global surge in demand for green packaging materials to maintain environmental cleanliness and reduce pollution [2]. These efforts aim to minimize reliance on petroleum-based plastics. Researchers are actively working to enhance biodegradable packaging plastics, advancing this innovative solution. Packaging materials provide physical protection and help create optimal physicochemical conditions for food. Key factors for improving biodegradable packaging include protecting food from oxygen, water vapor, ultraviolet

* *Corresponding author.*
E-mail address: basirah@uthm.edu.my

https://doi.org/10.37934/feel.1.1.4859

light, and both chemical and microbiological contamination [3]. New developments in packaging materials focus on extending food shelf life and ensuring consumer safety by reducing foodborne illnesses [4]. After their intended use, these materials should ideally biodegrade within a reasonable timeframe without causing environmental harm.

Starch has gained significant attention for its potential as a biodegradable thermoplastic polymer [5]. Agricultural products like starch offer a cost-effective and sustainable alternative for developing degradable materials. In Malaysia, sago starch derived exclusively from the Metroxylon sagu plant shows immense potential for creating biodegradable packaging materials. The properties of starch-based films and modification techniques for enhancing their physicochemical and mechanical characteristics have been extensively studied. This research uniquely highlights using sago starch (SS) as a promising material for producing innovative bioplastics reinforced with polysaccharide nanofillers. Nanotechnology involves manipulating materials at the nanometer scale to achieve desirable properties for novel applications [6]. Researchers have invested considerable effort in developing polymer-based nanocomposites, representing a breakthrough for biopolymer applications in the food packaging industry by addressing the limitations of traditional biodegradable plastics [7]. Incorporating nanofillers into biodegradable plastic films enhances their properties. Among these, chitosan (CS), a natural biopolymer, is frequently chosen due to its ease of synthesis, nontoxicity, biodegradability, biocompatibility, and cationic polysaccharide structure [8].

This study focuses on improving the physicochemical properties of sago starch–chitosan nanofiller films with additional polyvinyl alcohol (PVA) into the formulation, as well as developing new systems to extend their shelf life. These advancements align with the goal of preserving food using biodegradable packaging. The production of these bioplastics represents an economical and environmentally friendly approach to mitigating global pollution issues and ensuring sustainable future solutions.

2. Methodology

2.1 Optimization

Optimization of dependent variables was analyzed using Box-Behnken Design (BBD) from Design Expert 13.0 software as the statistical analysis may assess the effect of processing parameters on the response variables. Analysis of variance (ANOVA) statistically produced a set of data that comprised the probability of error (p-value) and F-value for the regression model and residual. A polynomial equation was developed from ANOVA data, which summarizes the interaction between the process parameters. An F-test was carried out to support the earlier results obtained from ANOVA.

2.1.1 Design of experiment

Levels of process parameters were determined to assess the optimization process. Table 1 portrays the range of factors used in the formulations of sago-based film. BBD was used to produce the same seventeen sets of experimental designs with different formulation ratios. Dependent variables, which consist of tensile strength and swelling index, were analyzed based on the experimental results. Statistical analysis was utilized to show the significance of the regression model and residuals and compare them with the F-test. The accuracy of the results was shown as the null hypothesis from the F-test was accepted. The interactions between factor variables were summarized into polynomial equations, Pareto charts, and response surface plots of process variables.

Table 1
Levels of independent variables for optimization process

Independent variables	Symbol	Range	Increment	Fixed Variable
SS (wt%)	X_1	$10 < X_1 < 90$	Δ40	Concentration of Sorbitol (Plasticizer)
CSN (wt%)	X_2	$20 < X_1 < 80$	Δ30	
PVA (wt%)	X_3	$20 < X_1 < 70$	Δ25	

3. Results and Discussion

3.1 Optimization by Response Surface Methodology (RSM)

The experimented response variables were analyzed based on the analysis of variance (ANOVA) at $p < 0.05$. The ANOVA was estimated to express the effects of linear, quadratic, and interaction coefficients on the responses. This part described the relationship between tensile strength and swelling index based on the quadratic model chosen to optimize the independent variables of SS, CSN, and PVA composition in a solution. In order to estimate the significance value of the model chosen, the F-value was used as the indicator to measure the confidence level obtained for the experimental design. The significant probability of error in the statistical analysis can be regarded as the p-value being higher than 0.05. The model was considered as significant as estimating a confidence level above 95 %. Based on the preliminary experiments, the optimization of process conditions was analyzed to determine the suitable conditions for synthesizing sago starch-based film (SBF). BBD was used to design the solution's experimental formulations of SS, CSN, and PVA composition. These variables were formulated and normalized based on basis of solutions at 100 wt %. BBD developed seventeen sets of experimental formulations with five replicates for the central point.

Table 2
ANOVA for tensile strength

Sources	Sum of Square	Degree of Freedom	Mean Squares	F-value	p-value
Model	2253.68	9	250.41	5.48	0.0177
Residual	319.63	7	45.66	-	-
Lack of fit	247.04	3	82.35	4.54	0.0890
Pure Error	72.58	4	18.15	-	-
Total	2573.31	16	-	-	-

The null hypothesis for the polynomial model was tested based on comparing the F-value. In order to test the null hypothesis of the polynomial model, the F-value calculated was compared to the F-value from the table. ANOVA produced an F-calculated value of 5.48. As for the F-tabulated value, it gained from the table based on the values obtained between the degree of freedom of regression, 9, and degree of freedom of residual, 7, at a 95 % confidence level. From table F critical points from Appendix A, the value of F-tabulated was 3.685. The condition was shown when F at (9, 7, 0.0177). The F-calculated value was higher than the F-tabulated value, which summed up to the null hypothesis for the response was accepted at a significance level, $\alpha = 5\%$. This indicates a good statistical analysis for tensile strength.

The analysis showed the model terms of X1, X2, X12, X22, X32, X1 X3 were significant for the analysis. Based on the coefficient estimate from the table, the values described the significance of each term in the formulation. The model terms were manipulated toward developing good tensile

strength of film plastic. Apart from that, the standard error illustrated the standard deviation for each term in the optimization process. Data analysis showed a small standard error for each, which can be summarized as a lower deviation from the mean values. Regression coefficient analysis revealed the actual values from the F-value and p-value for the model terms. The values regarded the probability of obtaining good data analysis from the process variables. Design Expert 13.0 software produced these statistical terms for the expression of coefficient interactions. It was then supported by a Pareto chart from Statsoft Statistica software to estimate the significance value for each model term.

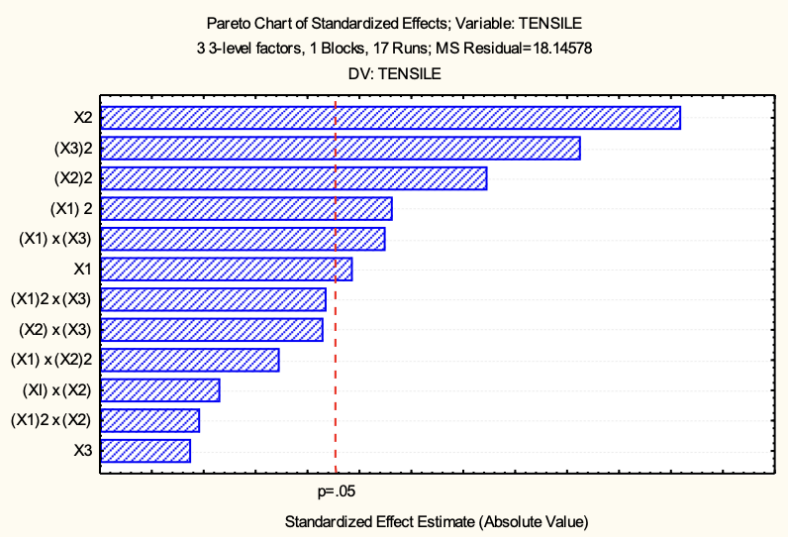

Fig. 1. Pareto chart of tensile strength

The Pareto chart plotted in Figure 1 portrays the significant model terms for the tensile strength. The most significant term in this response study was the linear term of CSN, X2; meanwhile, the second most significant estimation for the response was the quadratic term of PVA, X32. These process variables created good tensile strength conditions for the developed plastic. There were contributions of quadratic terms of CSN, X22 and SS, X12 respectively in accordance to increase the tensile strength of SBF. In addition, the interactions between SS and PVA in linear terms, X1 X3 ensure the decrement of brittleness for the plastic film. SS in linear terms was reported to provide a significant difference to tensile strength as it contained plasticizer to provide much higher strength for the plastic. The coefficients for the model terms were constructed in Equation 1.

$$Ytensile = 114.48 + 0.45\ X1 - 1.18\ X2 - 1.53\ X3 - (4.38\times10^{-3})\ X12 + (9.89\times10^{-3})\ X22 + 0.017\ X32 + (2.95\times10^{-3})\ X1\ X2 - (6.71\times10^{-3})\ X1\ X3 + (7.53\times10^{-3})\ X2\ X3 \quad (4.1)$$

ANOVA was crucial to the coefficient estimations as standard deviation and R2 value influenced the plotting. The analysis of tensile strength created a standard deviation of 6.76, revealing the actual average between the experimental data sets. The lower number of standard deviations indicates a good analysis of the response. The study of tensile strength granted the value of R2 at 0.8758 for this model. This implied a good correlation between the experimental and predicted value of the response. The developed model was considered statistically accurate by the estimated R2 value of more than 70% [9].

3.1.1.1 Analysis of response surface plot for tensile strength

Based on the Pareto chart, CSN played the most important role in developing good tensile strength of plastic. The linear terms of CSN showed a significant effect on the response as the p-value was lower than 0.05. The surface plot, as shown in Figure 2, portrayed the fitted response based on the factors of SS and CSN compositions. The figure showed the fluctuation of results due to undesirable factors. However, the results from the tensile strength analysis were then supported theoretically.

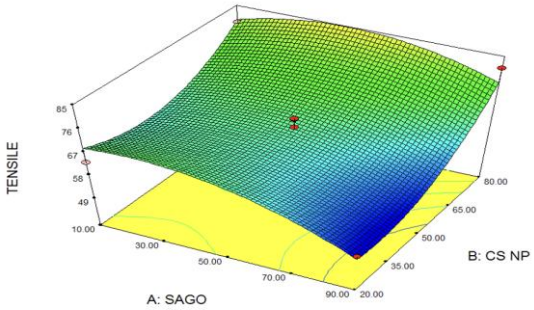

Fig. 2. Response surface plot of tensile strength as a function of SS and CSN

The highest tensile strength value was obtained from the interactions between the highest composition of CSN and a moderate amount of SS composition after five data replications. According to the response surface plot, as the CSN composition was increased to a low amount of SS composition, the tensile strength of the plastic increased dramatically. This happened due to nanofiller functions that can completely meet the requirements for experimental formulation. A higher SS composition in the formulations caused the excessive hydroxyl groups in the medium. Therefore, van der Waals forces took place due to higher hydroxyl groups [10-12]. The amide group of CSN was insufficient relative to the available hydroxyl group; hence, the bonding inside the film became weaker. The experimental results exhibited the values that followed the theory of chemical interactions.

The response surface plot in Figure 3 revealed the tensile strength value as a function of SS and PVA compositions. As the composition of SS and PVA increased, the film's tensile strength also increased. The phenomenon occurred due to hydrogen bonding inside the formulation. The molecular structure of SS and PVA allowed the H+ and OH- to interact [13-14]. There should be adequate SS and PVA compositions so that the interactions between the functional groups occur simultaneously.

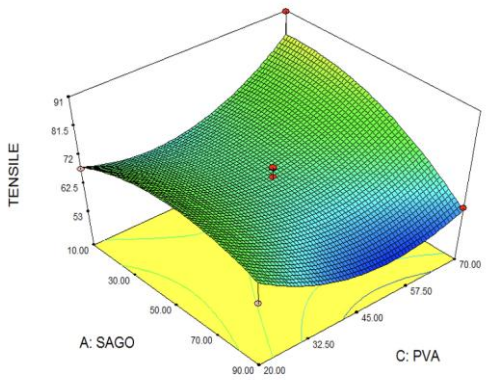

Fig. 3. Response surface plot of tensile strength as a function of SS and PVA

The interactions between CSN and PVA were summarized in the response surface plot in Figure 4. The findings were based on the compositions used in the film. As the composition of CSN and PVA increased, the developed film's tensile strength was also increased. The curvature shown in the surface plot provided information about interactions that should be in the correct ratio of compositions. The lowest ratio of both materials, which lay at 20 wt. % revealed a higher tensile strength of the plastic film. This concluded the composition ratio used in the solution was properly chosen for the formulations. Concentrations of process variables from the experimental designs were normalized into 100 wt % of solution basis. Therefore, the tensile strength of the plastic film was in the maximum state as the basis of the solution influenced the composition used in the solution.

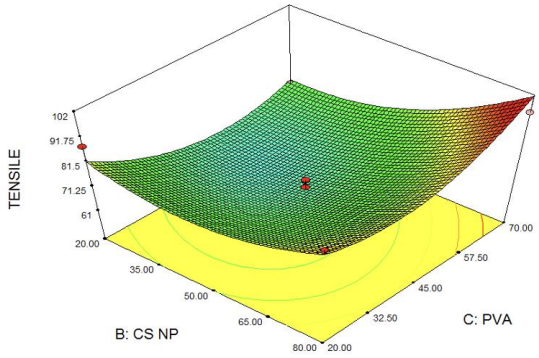

Fig. 4. Response surface plot of tensile strength as a function of CSN and PVA

3.1.2 Significance estimation for polynomial model of swelling index

ANOVA of the swelling index produced 0.0106 for p-value, which indicates the model terms were significant. Lack of fit showed the residual was insignificant in plotting the regression model as a p-value at 0.4719. ANOVA for the swelling index was tabulated in Table 3. After obtaining the significant value for the error probability, an F-test analysis was carried out.

Table 3
ANOVA for swelling index

Sources	Sum of Square	Degree of Freedom	Mean Squares	F-value	p-value
Model	4579.87	9	508.87	6.59	0.0106
Residual	540.25	7	77.18	-	-
Lack of fit	234.25	3	78.08	1.02	0.4719
Pure Error	306.00	4	76.50	-	-
Total	5120.12	16	-	-	-

F-values from mathematical and tabulated values were compared to test the null hypothesis for the polynomial model. The null hypothesis of the polynomial model was tested by comparison of F-calculated and F-tabulated values. ANOVA table constructed all the information about the response, which also expressed the value of F-calculated at 6.59. The f-tabulated value was the data obtained from the degree of freedom of regression, 9, and degree of freedom of residual, 7, at a 95 % confidence level. Table F critical points on Appendix A expressed the value of F-tabulated at F (9, 7, 0.0106) was 3.685. As ANOVA produced the value of F-calculated higher than the F-tabulated value, the conclusion for the F-test showed the null hypothesis was accepted at a significance level, α = 5%.

The analysis exhibited that X2 was the only significant model term. The Pareto chart for the swelling index response was constructed in Figure 5. This statistical chart supported the values obtained from the coefficient estimate value.

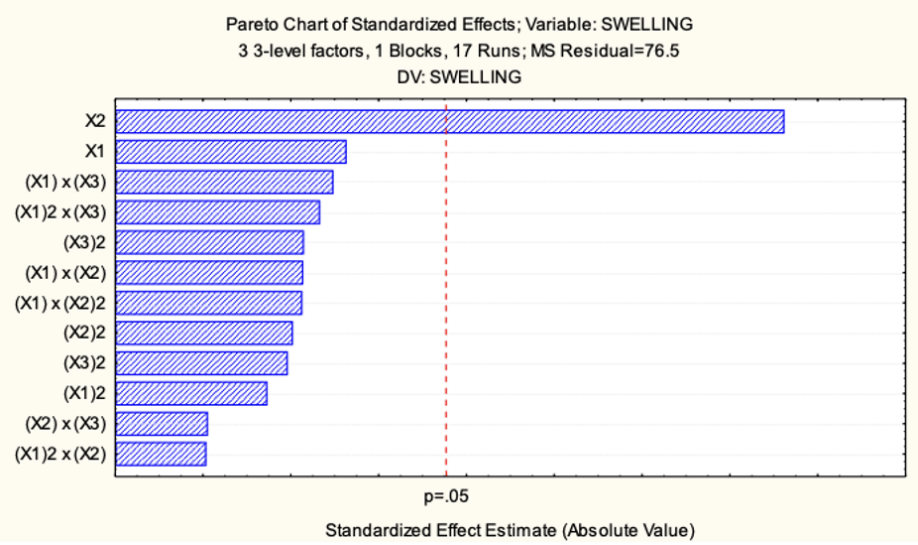

Fig. 5. Pareto chart of swelling index

The Pareto chart portrayed the significant coefficient terms for the swelling index. The most significant term in this response study was the linear term of CSN, X2. The explanation was about the chemical formula of CSN, which contained a phosphate group due to cross-linking. The interactions between CS and TPP may transform CSN into composite material. Therefore, the swelling for the SBF is influenced by the composition of CSN used in the solution. As the ratio of CSN increased, the swelling index gradually decreased. The actual coefficients for the model terms are explained in Equation 2. Positive and negative signs illustrated the dependency of response in boosting or depleting the process variables for producing good properties of plastic film.

Yswelling = 188.10392 - 0.53 X1 -1.43 X2 + 0.35 X3 + (1.95x10-3) X12 + (4.86x10-3) X22 - (6.60x10-3) X32 + (4.17x10-3) X1 X2 + (6.50x10-3) X1 X3 + (3.33x10-4) X2 X3 (4.2)

The analysis of the swelling index created a standard deviation of 8.79. The study of the swelling index produced the value of R2 at 0.8945. A good correlation between the experimental and predicted value of the response was shown based on the standard deviation and R2 value obtained from ANOVA. Polynomial response models were analyzed based on the quadratic model from the Box-Behnken design.

3.1.2.1 Analysis of response surface plot for swelling index

The Pareto chart showed the significance term of CSN (X2) as the variable prevented the water permeation into the plastic film. The linear term of CSN showed a significant effect on the response as the p-value was lower than 0.05. The response surface plot, as shown in Figure 4.6, portrayed the fitted response based on the factors of SS and CSN compositions. The experimental results exhibited a high degree of swelling as a low amount of CSN spread over the film. According to the figure, when the CSN composition was increased, the degree of swelling was gradually decreased. As CS undergoes the ionotropic gelation with TPP, the phosphate group will be attached to each nanoparticle [15-17].

The environment created non-polar particles as the NH3+ interacts with PO4- [18-20]. Thus, it will induce protection against the permeation of water into the film.

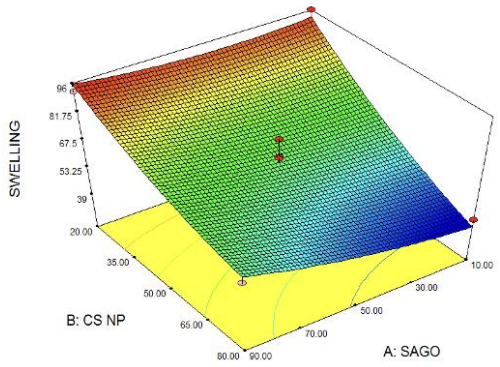

Fig. 6. Response surface plot of swelling index as a function of SS and CSN

The response surface plot in Figure 7 exhibited the value of the swelling index as a function of SS and PVA compositions. As the composition of SS and PVA increased, the swelling index of plastic films also increased. Maximum degrees of swelling were achieved as the SS and PVA compositions were at the maximum state. Biocomposite plastic gradually swelled up as it was immersed in deionized water. This phenomenon happened due to hydrogen bonding between SS and PVA which allowed the permeation of water into the film. Water molecules also provided the hydroxyl group, hence the polarity may cause the molecules to interact through hydrogen bonding [21].

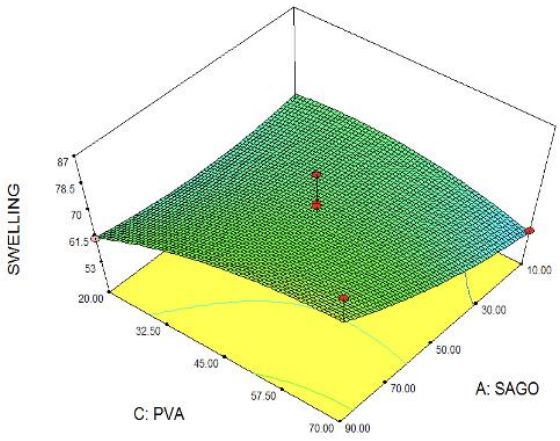

Fig. 7. Response surface plot of swelling index as a function of SS and PVA

The interactions between CSN and PVA were summarized in the response surface plot in Figure 8. The findings were based on the compositions used in the film. At a high composition of CSN, the degree of swelling for the plastic films was steadily low. A similar condition happened as the CS was transformed into nanoparticles; the crosslinking agent of TPP allowed the formation of non-polar nanoparticles. The phenomenon induced to composite blending of CSN into the film solution. The plotting was theoretically accurate since it revealed that nanofillers were sufficient to be dispersed in the solution, which consequently conferred a low swelling index.

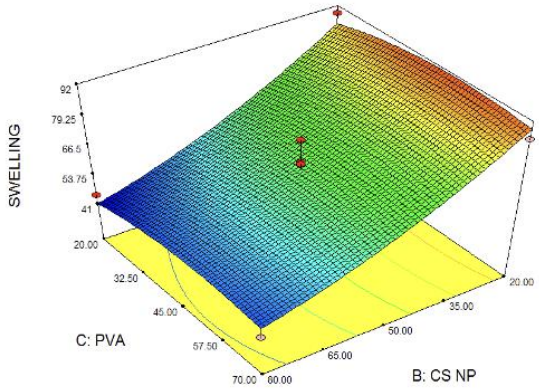

Fig. 8. Response surface plot of swelling index as a function of CSN and PVA

3.1.3 Multiple response optimization

Optimization of biocomposite plastic film required maximum tensile strength and minimum swelling index values. Therefore, the goals for process variables and responses were estimated during the analysis in the initial statistical analysis phase. The range of conditions for the independent variables was set into 'in range' values using the numerical optimization function of Design Expert 13.0. The lower and upper limits for independent and dependent variables were determined based on preliminary experiments and ANOVA. Preliminary experiments helped to evaluate the range of levels from the experimental results, whereas ANOVA measured the significant value of model terms. There should be optimum conditions for developing SBF. Statistical analysis from the software produced a set of optimum conditions for those three independent variables. Table 4 shows the optimized values for process variables and response values with high desirability functions. Based on the tabulated values, it revealed that SBF demanded CSN in high composition as the parameter may trigger toward high tensile strength and low swelling index. The expected value for tensile strength was as much as 95.98 MPa, whereas the swelling index was expected to be low for up to 38.07 %.

Table 4
Optimum values for variables

Parameters	Goal	Optimum Values
SS	In range	21.73
CSN	In range	78.50
PVA	In range	64.18
Tensile Strength	Maximize	95.98
Swelling Index	Minimize	38.07

Figure 9 explains the ramp function graph of desirability for tensile strength and swelling index. The ramp for each variable was designed based on the conditions selected earlier in the experimental design. Point on the ramps illustrated the optimized value gained from statistical analysis. As the process variables were manipulated, the experimental values from both responses reflected the compositions needed to be used for the formulations of film and gave the expected results for the process of re-synthesis of film.

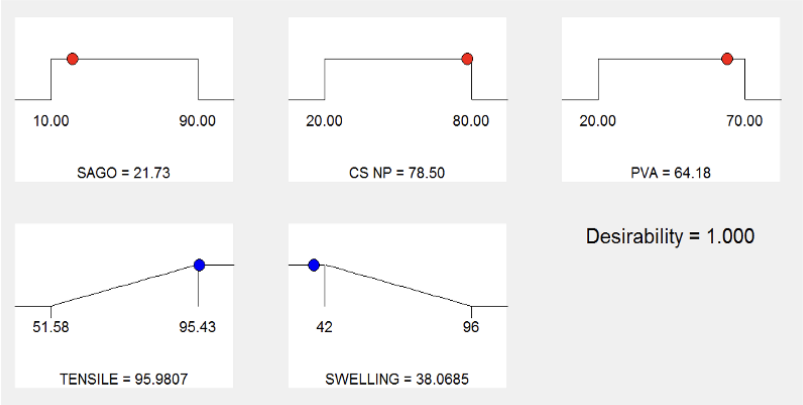

Fig. 9. Ramp function graph of desirability for responses

The histogram in Figure 10 presented the overall desirability function of tensile strength and swelling index. Desirability ranged from 0 to 1, as parameters were measured to determine the optimum conditions for the formulations. In addition, the functionality of desirability could be the turning point to understanding the closeness of the response to the desired outcome. The study obtained the maximum desirability which summarized the whole statistical analysis was in good condition. In explanation, the statistical analysis from this optimization process served a good quality of process using those three process variables. Based on the experimental results from seventeen sets of data, it concluded that the aim of the study was to obtain the maximum tensile strength and minimum swelling index. Therefore, the selection of the process variables range was on target as it produced the optimized SS, CSN, and PVA values, which can provide the desired values for both responses. The graph showed the desirability of process variables and responses, and their combination was 1. This condition indicates the maximum desirability obtained from the statistical analysis.

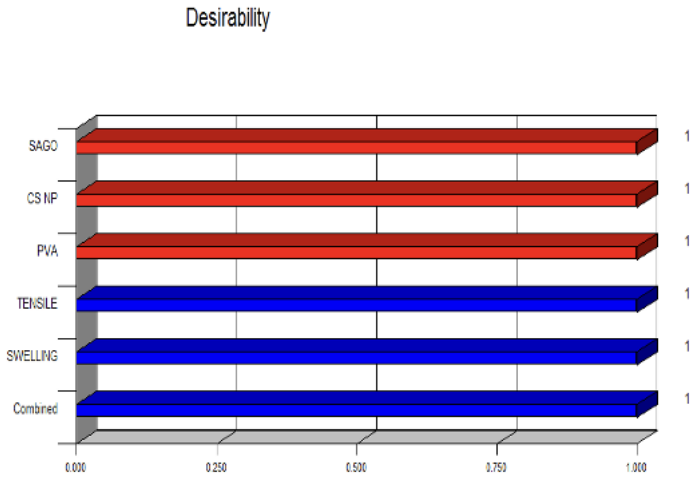

Fig. 10. Histogram of desirability for tensile strength and swelling index

The statistical analysis of the film formulations demonstrated significant results for the selected model in the optimization process. In the BBD quadratic two-way interaction, the p-value for tensile strength is 0.0177 at a 95% confidence level. Similarly, the swelling index yielded a p-value of 0.0106, indicating significance at $p < 0.05$. These values confirm the reliability of the findings regarding tensile strength and swelling properties, underscoring the validity of the analysis. The optimized values

derived from the statistical analysis were subsequently re-synthesized to ensure accuracy in the final characterization results.

Acknowledgement
Communication of this research is made possible through monetary assistance by Universiti Tun Hussein Onn Malaysia and the UTHM Publisher's Office via Publication Fund E15216.

References

[1] Avella, M., De Vlieger, J. J., Errico, M. E., Fischer, S., Vacca, P., and Volpe, M. G. (2005). "Biodegradable starch/clay nanocomposite films for food packaging applications," *Food Chemistry* 93(3), 467-474. DOI: 10.1016/j.foodchem.2004.10.024
[2] Oleyaei, S. A., Zahedi, Y., Ghanbarzadeh, B., and Moayedi, A. A. (2016). "Modification of physicochemical and thermal properties of starch films by incorporation of TiO2 nanoparticles," International Journal of Biological Macromolecules 89, 256-264. DOI: 10.1016/j.ijbiomac.2016.04.078
[3] Prasad, P., and Kochhar, A. (2014). "Active packaging in food industry: A review," *Journal of Environmental Science, Toxicology and Food Technology* 8(5), 1-7. DOI: 10.9790/2402-08530107
[4] Caro, N., Quiñonez, E. M., Díaz-Dosque, M., López, L., Abugoch, L., and Tapia, C. (2015). "Novel active packaging based on films of chitosan and chitosan/quinoa protein printed with chitosan-tripolyphosphate-thymol nanoparticles via thermal ink-jet printing," *Food Hydrocolloids* 52, 520-532. DOI: 10.1016/j.foodhyd.2015.07.028
[5] Lu, Y., Weng, L., and Cao, X. (2006). "Morphological, thermal and mechanical properties of ramie crystallites-reinforced plasticized starch biocomposites," *Carbohydrate Polymers* 63(2), 198-204. DOI: 10.1016/j.carbpol.2005.08.027
[6] Huang, J.-Y., Li, X., and Zhou, W. (2015). "Safety assessment of nanocomposite for food packaging application," *Trends in Food Science & Technology* 45(2), 187-199. DOI: 10.1016/j.tifs.2015.07.002
[7] Abdollahi, M., Alboofetileh, M., Rezaei, M., and Behrooz, R. (2013). "Comparing physico-mechanical and thermal properties of alginate nanocomposite films reinforced with organic and/or inorganic nanofillers," *Food Hydrocolloids* 32(2), 416-424. DOI: 10.1016/j.foodhyd.2013.02.006
[8] Onishi, H., and Machida, Y. (1999). "Biodegradation and distribution of water-soluble chitosan in mice," *Journal of Biomaterials* 20(2), 175-182. DOI: 10.1016/S0142-9612(98)00159-8
[9] Meynard, Christine N. and David M. Kaplan, 2011. "The effect of a gradual response to the environment on species distribution modeling performance", Ecography (6), 35:499-509. DOI: 10.1111/j.1600-0587.2011.07157.x.
[10] Gao, Feng, Zhifu Shen, Zhihua Wang, Hongmei Gao, and Lu Liu, 2020. "Numerical integration of van der waals force between clay plates", Japanese Geotechnical Society Special Publication(2), 8:23-26. https://doi.org/10.3208/jgssp.v08.c23
[11] Rachmawati, Ika Yuni, 2024. "Investigation on the collection mechanism of van der waals force in air filtration by numerical simulation and empirical model development", Industrial & Engineering Chemistry Research(23), 63:10410-10426. https://doi.org/10.1021/acs.iecr.4c00550
[12] Sasihithlu, Karthik, J. B. Pendry, and R. V. Craster, 2017. "van der waals force assisted heat transfer", Zeitschrift Für Naturforschung A(2), 72:181-188. https://doi.org/10.1515/zna-2016-0361
[13] Jose, Jobin, Mamdouh A. Al-Harthi, Mariam Al-Ali AlMaadeed, Jolly Bhadra Dakua, and S. K. De, 2015. "Effect of graphene loading on thermomechanical properties of poly(vinyl alcohol)/starch blend", Journal of Applied Polymer Science(16), 132. https://doi.org/10.1002/app.41827
[14] Shrestha, Binod, Khagendra Chapain, Sambridhi Shah, and Rajesh Pandit, 2023. "starch/ polyvinyl alcohol (pva) blend bioplastics: synthesis and physicochemical properties", Journal of Nepal Chemical Society(2), 43:103-109. https://doi.org/10.3126/jncs.v43i2.53349
[15] Costa, Eduardo M., Sara Silva, and Manuela Pintado, 2023. "Chitosan nanoparticles production: optimization of physical parameters, biochemical characterization, and stability upon storage", Applied Sciences(3), 13:1900. https://doi.org/10.3390/app13031900
[16] Meena, Mahendra, 2024. "A novel histidine functionalized chitosan nanoformulation: synthesis, characterization and its bioactivity in tomato plant",. https://doi.org/10.21203/rs.3.rs-4002182/v1
[17] Rietra, R.P.J.J., Tjisse Hiemstra, and W.H. van Riemsdijk, 2001. "interaction between calcium and phosphate adsorption on goethite", Environmental Science & Technology(16), 35:3369-3374. https://doi.org/10.1021/es000210b

[18] Kouchak, Maryam and Armita Azarpanah, 2015. "Preparation and in vitro evaluation of chitosan nanoparticles containing diclofenac using the ion-gelation method", Jundishapur Journal of Natural Pharmaceutical Products(2), 10. https://doi.org/10.17795/jjnpp-23082

[19] Pedroso-Santana, Seidy and Noralvis Fleitas-Salazar, 2020. "ionotropic gelation method in the synthesis of nanoparticles/microparticles for biomedical purposes", Polymer International(5), 69:443-447. https://doi.org/10.1002/pi.5970

[20] Goycoolea, Francisco M., Fabrice Brunel, Nour Eddine El Gueddari, Anna Coggiola, Giovanna Lollo, Bruno M. Moerschbacher, Carmen Remuñán-López et al., 2016. "Physical properties and stability of soft gelled chitosan-based nanoparticles", Macromolecular Bioscience(12), 16:1873-1882. https://doi.org/10.1002/mabi.201600298

[21] Hong, Seungpyo and Dongsup Kim, 2015. "interaction between bound water molecules and local protein structures: a statistical analysis of the hydrogen bond structures around bound water molecules", Proteins Structure Function and Bioinformatics(1), 84:43-51. https://doi.org/10.1002/prot.24953